Escaping the Krylov space during finite-precision Lanczos

Jannis Eckseler,[1,*] Max Pieper,[1,†] and Jürgen Schnack[1,‡]

[1] *Fakultät für Physik, Universität Bielefeld, Postfach 100131, D-33501 Bielefeld, Germany*

(Dated: July 23, 2025)

The Lanczos algorithm, introduced by Cornelius Lanczos, has been known for a long time and is widely used in computational physics. While often employed to approximate extreme eigenvalues and eigenvectors of an operator, recently interest in the sequence of basis vectors produced by the algorithm rose in the context of Krylov complexity. Although it is generally accepted and partially proven that the procedure is numerically stable for approximating the eigenvalues, there are numerical problems when investigating the Krylov basis constructed via the Lanczos procedure. In this paper, we show that loss of orthogonality and the attempt of reorthogonalization fall short of understanding and addressing the problem. Instead, the sequence of numerical Lanczos vectors in finite-precision arithmetic escapes the true vector space spanned by the exact Lanczos vectors. This poses the real threat to an interpretation in view of the operator growth hypothesis.

Keywords: Krylov complexity, Lanczos algorithm

I. INTRODUCTION

The Lanczos procedure [1] is applied in many contexts in physics for instance to approximate extreme eigenvalues of operators such as ground states and low-lying excited states of Hamiltonians as well as functions of the Hamiltonian such as the partition function, compare e.g. [2–10]. Its accuracy has been thoroughly investigated over time with the general result that the method is very accurate and robust in finite precision arithmetics which is an important issue for computer applications [11–19].

Recent efforts to understand the emergence of thermodynamics in closed quantum systems under unitary time evolution [20–36] produced a variety of measures to discriminate between, e.g., integrable and quantum chaotic behavior such as *level statistics* (Poisson vs. Wigner-Dyson) and *Thouless time* to mention just two of them [37, 38]. A new approach to separate quantum chaotic dynamics from the dynamics of integrable quantum systems is given by the *universal operator growth hypothesis* [36] which heavily relies on the Lanczos procedure and thus sparked new and intensified interest in the Lanczos algorithm applied to finite size systems as well as to systems in the thermodynamic limit [39–50]. The hypothesis links the asymptotic behavior of the Lanczos coefficients to the characteristic of integrability of the system. However in the process of calculating these coefficients, numerical difficulties can occur.

In our investigation, we show that the numerical sequence of eigenvectors in finite precision arithmetic escapes the true vector space spanned by the exact Lanczos vectors. The underlying reason is that this space is embedded in the much larger computational vector space. We think that loss of orthogonality to previous Lanczos vectors is a minor problem compared to acquiring components into the Lanczos sequence that do not belong to the true space. These components grow exponentially fast which is a genuine property of the Lanczos procedure. This numerical problem cannot be cured by reorthogonalization. Therefore, the interpretation of numerical Lanczos sequences in view of the operator growth hypothesis appears questionable to us.

The paper is organized as follows: In Section II we recapitulate essentials of the Lanczos procedure, and in Section III we discuss and demonstrate with a few examples of finite quantum spin systems how the mentioned numerical problems arise. The paper closes with a summary. In the appendix, we demonstrate with two examples that the identified problems also arise in ordinary Lanczos procedures for ket states or wave functions.

II. LANCZOS ALGORITHM AND THE OPERATOR GROWTH HYPOTHESIS

Since the operator growth hypothesis makes a statement about the Lanczos coefficients we first have to review the Lanczos algorithm [1]. To start the Lanczos algorithm one needs a linear operator H and a normalized starting vector $|\,\psi\,\rangle$ or, when considering the Hilbert space of operators, a starting operator $|\,O\,)$ and a superoperator $\mathcal{L}$ [51]. This Hilbert space of operators has to be provided with an inner product, which in this paper is chosen to be the infinite temperature product $(\,A\,|\,B\,) = Tr(A^\dagger B)/dim(\mathcal{H})$, also known as the Frobenius product, with the induced norm $||A|| = \sqrt{(\,A\,|\,A\,)}$. Note that, since the Hilbert space of operators is also a vector space, we might call operators vectors as well. However, the distinction between vectors in the ket-vector space $\mathcal{H}$ and the operator-vector space $\mathcal{H}\otimes\mathcal{H}$ will be made clear by different notations as $|\,v\,\rangle$ and $|\,w\,)$, respectively. For physical systems the linear superoperator of interest is the Liouvillian $\mathcal{L}$ which is defined via $\mathcal{L}\,|\,O\,) = [H, O]$ where H is the Hamiltonian of the system. To start the Lanczos algorithm we set $|\,O_0\,) = |\,O\,)$,

* jeckseler@physik.uni-bielefeld.de
† mpieper@physik.uni-bielefeld.de
‡ jschnack@uni-bielefeld.de

$b_1 = ||\mathcal{L}O_0||$, and $|\,O_1\,) = b_1^{-1} L\,|\,O_0\,)$. We then follow the iteration scheme

$$|\,A_n\,) = \mathcal{L}\,|\,O_{n-1}\,) - b_{n-1}\,|\,O_{n-2}\,) \tag{1}$$

$$b_n = ||A_n|| \tag{2}$$

$$|\,O_n\,) = b_n^{-1}\,|\,A_n\,) \tag{3}$$

to construct the Krylov basis $\{|\,O_n\,)\}$, which is an ONB of the Krylov space. Note that since we are considering a starting vector $|\,O\,)$, which is a hermitian operator, one only needs to project out the second latest $|\,O_n - 2\,)$, because the inner product $(\,O_n - 1\,|\,\mathcal{L}O_n - 1\,)$ vanishes for hermitian and skewhermitian operators O.

In exact arithmetic the Lanczos algorithm works just as described, however with finite numerical precision the constructed $|\,O_n\,)$ are generally not an ONB. While for many applications of the Lanczos algorithm this does not pose a problem, it is crucial in our case, since it can heavily influence the Lanczos sequence. A usual attempt at trying to better the results is to reorthogonalize with respect to all prior operators, so all $|\,O_k\,)$ with $k < n$ or even repeat the reorthogonalization procedure a second time as suggested in [52], which we call double reorthogonalization. While this may lead to termination of the Lanczos sequence in some cases, there are still numerical problems, which will be discussed in section III.

The Liouvillian in the Krylov basis is a tridiagonal matrix of the form

$$\mathcal{L} = \begin{pmatrix} 0 & b_1 & 0 & 0 & \cdots & \cdots & 0 \\ b_1 & 0 & b_2 & 0 & \cdots & \cdots & 0 \\ 0 & b_2 & 0 & b_3 & \cdots & \cdots & 0 \\ \vdots & & \ddots & \ddots & \ddots & & \vdots \\ 0 & \cdots & \cdots & b_{m-3} & 0 & b_{m-2} & 0 \\ 0 & \cdots & \cdots & 0 & b_{m-2} & 0 & b_{m-1} \\ 0 & \cdots & \cdots & 0 & 0 & b_{m-1} & 0 \end{pmatrix}, \tag{4}$$

with $\mathcal{L}_{mn} = (\,O_m\,|\,\mathcal{L}\,|\,O_n\,)$. The Lanczos coefficients b_n are the quantity of interest for the universal operator growth hypothesis, which states that for infinite nonintegrable systems and a local starting operator O these b_n should grow asymptotically linearly with n.

III. NUMERICAL PROBLEMS IN FINITE SYSTEMS

While originally formulated for infinite systems, there has also been interest in the behavior of the Lanczos sequence in finite systems. Obviously, the universal operator growth hypothesis cannot hold for finite systems since the Lanczos sequence will terminate at some point and can therefore not grow asymptotically linearly. However one can still examine the Lanczos sequence up to that point and compare the behavior in different systems [52, 53].

It is known that the dimension of the Krylov space $\mathcal{K}(\mathcal{L}, O) = span\{|\,O\,), \mathcal{L}\,|\,O\,), \mathcal{L}^2\,|\,O\,), ...\}$ is the minimum number of eigenvectors of $\mathcal{L}$ needed to represent the starting vector $|\,O\,)$. Therefore, if the system is small enough to diagonalize it computationally, one can predict the actual Krylov space dimension. This is a useful insight to show that numerically the Lanczos sequence does not terminate at the edge of the Krylov space. In exact arithmetic the b_n should vanish for $n_{\max} = dim(\mathcal{K}(\mathcal{L}, O)) + 1$ since at $n_{\max} - 1$ we already constructed a full ONB for the Krylov space at hand. Iterating one more step should yield an operator A_n with $||A_n|| = 0$, hence $b_n = 0$.

A. Tilted-field Ising ring

To numerically investigate this behavior we considered the tilted-field Ising model given by the Hamiltonian

$$H = \sum_{i=0}^{N-1} s_i^z s_{i+1}^z + h_z s_i^z + h_x s_i^x\ , \tag{5}$$

where we used periodic boundary conditions and chose $N = 6$, $h_z = 1$ as well as $h_x = -1.05$. The starting vector for which the Lanczos method is applied was chosen to be the 1-local operator s_0^z.

In order to compute the dimension of the Krylov space $\mathcal{K}(\mathcal{L}, s_0^z)$ one first has to find the eigenvectors $|\,E_k^{\mathcal{L}}\,)$ and eigenvalues $E_k^{\mathcal{L}}$ of $\mathcal{L}$. This can either be done by diagonalizing $\mathcal{L}$ itself or by diagonalizing H to obtain its eigenvalues E_m^H and eigenvectors $|\,E_m^H\,\rangle$, and using these to construct an eigenvector and eigenvalue of $\mathcal{L}$ via

$$|\,E_{k(m,n)}^{\mathcal{L}}\,) = |\,E_m^H\,\rangle\langle\,E_n^H\,| \text{ and } E_{k(m,n)}^{\mathcal{L}} = E_m^H - E_n^H\,, \tag{6}$$

where $k(m,n)$ is the integer enumeration for the eigenstates of the Liouvillian

Now let $\{E_p^{\mathcal{L}}\}$ be the set of eigenspaces of $\mathcal{L}$. Then the starting vector $|\,s_0^z\,)$ can be decomposed as

$$|\,s_0^z\,) = \sum_{p=1}^{\#\{E_p^{\mathcal{L}}\}} d_p \sum_{k=1}^{dim(E_p^{\mathcal{L}})} c_k^p\,|\,E_{k,p}^{\mathcal{L}}\,)\ . \tag{7}$$

One can represent the second sum as one combined vector $|\,\bar{E}_p^{\mathcal{L}}\,) = \sum_{k=1}^{dim(E_p^{\mathcal{L}})} c_k^p\,|\,E_{k,p}^{\mathcal{L}}\,)$, which are the only eigenvectors needed to represent our starting vector in this eigenspace, such that we can now write

$$|\,s_0^z\,) = \sum_{p=1}^{\#\{E_p^{\mathcal{L}}\}} d_p\,|\,\bar{E}_p^{\mathcal{L}}\,)\ . \tag{8}$$

As mentioned before, the dimension of $\mathcal{K}(\mathcal{L}, s_o^z)$ is just the number of eigenvectors to different eigenvalues that $|\,s_0^z\,)$ has an overlap with, so the number of coefficients d_p with $d_p \neq 0$.

In Fig. 1 it can be seen that the reorthogonalized Lanczos sequence does not terminate when the full dimension ($dim(\mathcal{K}) = 1893$, indicated by the blue vertical

line) of the Krylov space is reached. To further investigate whether a vector $|\,O_n\,)$ lays partially outside of the Krylov space one can consider the decomposition of $|\,O_n\,)$ into the $|\,\bar{E}_p^{\mathcal{L}}\,)$

$$|\,O_n\,) = \sum_{p=1}^{dim(\mathcal{K})} d_p^n\,|\,\bar{E}_p^{\mathcal{L}}\,)\;. \tag{9}$$

Since this also builds an ONB for the Krylov space, one can check whether the overlap of the newly generated vector $|\,O_n\,)$ with the given ONB $\{|\,\bar{E}_p^{\mathcal{L}}\,)\}$ is still unity, thus showing that the operator is still completely contained within the Krylov space. The overlap with the Krylov space is given by

$$C_n = \sqrt{\sum_{p=1}^{dim(\mathcal{K})} (d_p^n)^2} = \sqrt{\sum_{p=1}^{dim(\mathcal{K})} (\,O_n\,|\,\bar{E}_p^{\mathcal{L}}\,)^2}\;. \tag{10}$$

This is shown by the green curve in Fig. 1.

Since a drop of C_n at around $n = 100$ can be observed it shows that the Lanczos sequence is no longer completely contained within the Krylov space quite early compared to the predicted dimension. This shows that in general the Krylov space is numerically not closed under the Lanczos algorithm. It should be noted at this point that the diagonalization as well as the decomposition of the operators into the eigenbasis of $\mathcal{L}$ is done numerically. Therefore, in section III B we will present a case where the eigenbasis is known analytically and artifacts of a numerical diagonalization can be excluded.

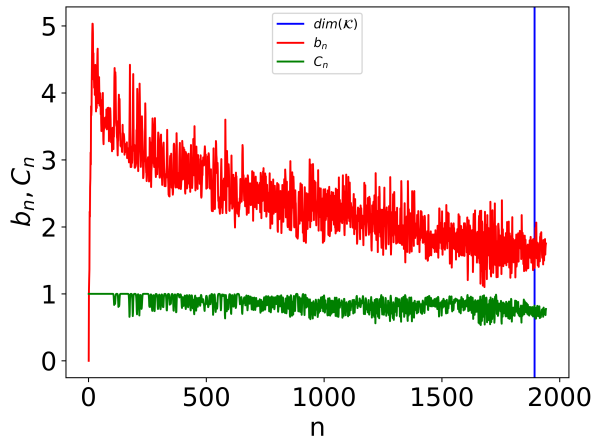

Figure 1. Lanczos sequence b_n with double reorthogonalization and overlap C_n for the tilted-field Ising ring with the starting vector $|\,s_0^z\,)$. The blue line is drawn at the numerically known dimension of the Krylov space $dim(\mathcal{K}) = 1893$.

In order to estimate the impact of the numerical accuracy on the calculation presented in Fig. 1 we repeated the calculation originally done in C++ with *double* floats now with *float* as well as *long double*. The example showed that *float* is absolutely untrustworthy; it produced much larger errors and a massively too large estimate of the dimension. This should be a warning to everyone still using graphics cards with float precision. The more precise calculations with *long double* yielded the same predicted dimension as for *double*, similar b_n, and slightly later dropping C_n (only 10 more steps). However, the usage of *long double* allows for more precise tuning of the tolerance parameter in distinguishing degeneracies of the Liouvillian.

Using a representation of the Liouvillian and the Lanczos vectors $|\,O_n\,)$ which is constrained to the Krylov space can remove the possibility of leaving $\mathcal{K}$ during the Lanczos procedure. This is done by considering the decomposition Eq. (9) and calculating the matrix representation of $\mathcal{L}$ via

$$\mathcal{L}^{\mathcal{K}}_{k,k'} = (\,\bar{E}_k^{\mathcal{L}}\,|\,\mathcal{L}\,|\,\bar{E}_{k'}^{\mathcal{L}}\,)\;. \tag{11}$$

Obviously, this is a diagonal matrix, however, it is not the entire diagonal matrix of $\mathcal{L}$ in the complete Hilbert space, since it does not contain the degeneracies of eigenvalues or eigenspaces that do not appear in the decomposition of the starting vector. Doing the Lanczos iterations with this $dim(\mathcal{K})\times dim(\mathcal{K})$ matrix and the $dim(\mathcal{K})$-dimensional vector following from Eq. (9) then leads to Fig. 2.

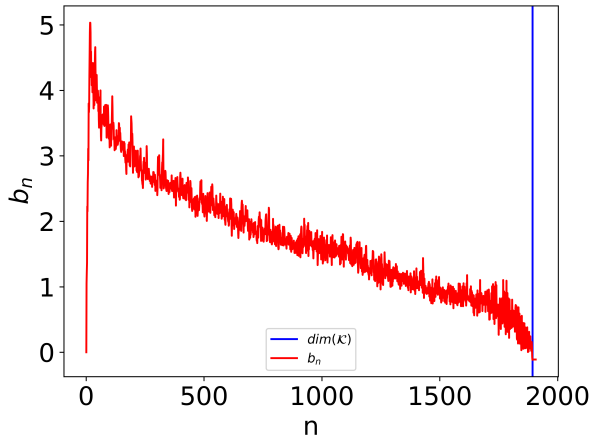

Figure 2. Lanczos sequence b_n with double reorthogonalization and a representation constrained to the Krylov subspace for the tilted-field Ising ring with the starting vector $|\,s_0^z\,)$. The blue line is drawn at the numerically known dimension of the Krylov space $dim(\mathcal{K}) = 1893$.

Now the Lanczos sequence terminates at the Krylov space dimension. This is no surprise, since we chose a representation which enforces this behavior. Nonetheless, we eliminated the effect of leaving the Krylov space during the Lanczos procedure. It should be noted however that a lot of extra computational effort had to be made for this, because we need to diagonalize $\mathcal{L}$, represent our starting operator with respect to its eigenvectors $|\,E_k^{\mathcal{L}}\,)$ and numerically distinguish non-degeneracy of the eigenvalues. Even though this way the resulting b_n seem better, in the sense that there are no artifacts of leaving the Krylov space, we still can not say that they are

definitely closer to the 'true' b_n at all iteration steps. In Fig. 3 the Lanczos sequence is shown for different methods of calculation. One can see that for the single and double reorthogonalization the b_n are closer to the case of a constrained representation. However, the problem of non-vanishing b_n at $dim(\mathcal{K})$ is still visible.

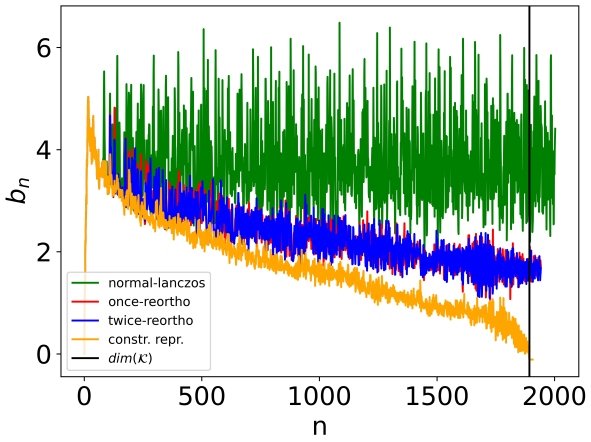

Figure 3. Lanczos sequence b_n calculated with different methods for the tilted field Ising ring with the starting operator s_0^z. The constrained representation (constr. repr.) means a representation of the Liouvillian according to Eq. (11). The black line is drawn at the calculated dimension of the Krylov space $dim(\mathcal{K}) = 1893$.

B. One magnon space of the Heisenberg delta chain

All of this can already be seen when considering a small symmetry-related subspace of a Hilbert space. For this purpose, we consider the $(M = Ns - 1)$-subspace of the antiferromagnetic Heisenberg delta chain given by the Hamiltonian

$$H = J_1 \sum_{i=0}^{N-1} \vec{s}_i \cdot \vec{s}_{i+1} + J_2 \sum_{i=0}^{\frac{N}{2}-1} \vec{s}_{2i} \cdot \vec{s}_{2i+2} \ , \tag{12}$$

which has a flat band for the case of $J_2/J_1 = 1/2$, see [54] and references therein. The Hamiltonian in this small subspace can be diagonalized analytically leading to the eigenvalues of H

$$E_0^H = \frac{NJ_1}{4} + \frac{NJ_2}{8} - 4J_2 \tag{13}$$

$$E_1^H = \frac{NJ_1}{4} + \frac{NJ_2}{8} - J_2 \left[1 - \cos\left(\frac{4\pi k}{N}\right)\right], \tag{14}$$

which can be used to calculate the eigenvalues of the Liouvillian via (6). The eigenvectors of H and thus of $\mathcal{L}$ are also known analytically. If one takes as a starting operator a chosen superposition of these eigenvectors, it is no longer a question of numerical accuracy to find the minimal number of eigenvectors of $\mathcal{L}$ needed to represent the starting operator. To make sure we do not use degenerate eigenvectors we only use those constructed by the tensor product $|\,E^H_{0,k=0}\rangle\langle\,E^H_{1,k'}\,| \;=\; |\,E^{\mathcal{L}}_m\,)$ with $k' < \frac{N}{4}$ (see Fig. 4), thus leading to a strictly monotonic increase in $E^{\mathcal{L}}_{m(k-k')} = E^H_{0,k=0} - E^H_{1,k'}$ with k'. In addition to these eigenvectors, we also include the adjoint of every vector $|\,E^H_{1,k'}\rangle\langle\,E^H_{0,k=0}\,| \;=\; |\,E^{\mathcal{L}\dagger}_m\,)$ in order to later construct a hermitian operator as a starting vector in this subspace. These adjoined eigenvectors are not degenerate, as adjoining the vectors introduces a sign change in their energies $E^{\mathcal{L}}_{m(k'-k)} = -E^{\mathcal{L}}_{m(k-k')}$.

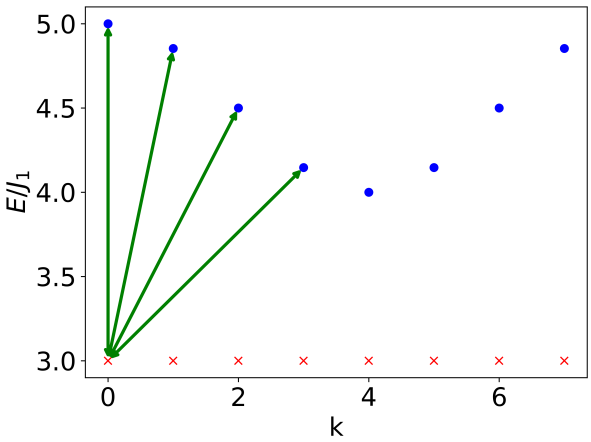

Figure 4. One magnon band structure of the Heisenberg delta chain for $N = 16$ and choice of eigenvectors used for the tensor product. Note that the arrows point in both directions.

Choosing now a uniform superposition of these eigenvectors and their adjoint counterparts

$$|\,A\,) = \sqrt{\frac{4}{N}} \sum_{m=0}^{N/4-1} (\,|\,E^{\mathcal{L}}_m\,) + |\,E^{\mathcal{L}\dagger}_m\,)) \tag{15}$$

in an example case of $N = 500$ leads to an analytically known dimension and basis of the Krylov space of $dim(\mathcal{K}) = 250$. It should be noted that the operator we constructed this way is hermitian but not necessary local or of any obvious physical meaning. However, one can still execute the Lanczos algorithm and investigate if the sequentially constructed vectors partially leave the Krylov space. Computing the Lanczos algorithm for this system and starting vector leads to the sequence shown in Fig. 5.

Again it is visible that the vectors leave the Krylov space at around $n = 55$ where C_n drops from one. The b_n show some strongly alternating behavior, It could be speculated that these oscillations are related to the flat band in our example. We refer interested readers to [55]. But since we do not consider a local or even physical starting operator the alternating behavior is not necessarily of any bigger meaning.

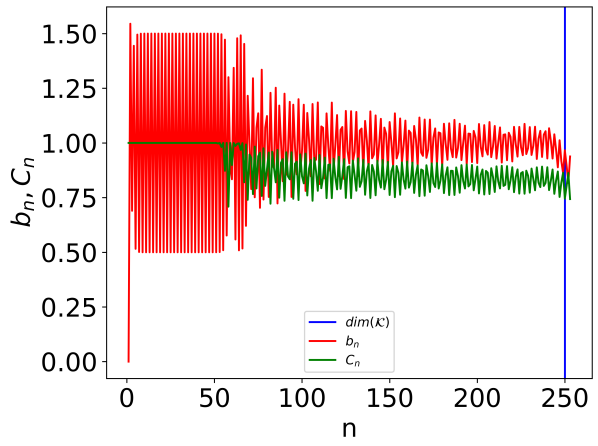

Figure 5. Lanczos sequence b_n and overlap C_n for the one-magnon space of the Heisenberg delta chain with the starting vector $|A\rangle$. The blue line is drawn at the analytically known dimension of the Krylov space $dim(\mathcal{K}) = 250$.

IV. SUMMARY

In this paper we showed that vectors generated numerically via the Lanczos algorithm do not need to reside in the Krylov space of the starting vector. This might even be of advantage for some applications like finding the eigenvalues of an operator, since as shown in appendix A even when starting with a vector which does not have an overlap with the ground state it might still be reached numerically. However, in situations where one fine tunes this starting vector to only have an overlap with some of the eigenvectors of the considered Hamiltonian or Liouvillian it is not guaranteed that it will stay inside the corresponding Krylov space. Especially for the operator Lanczos discussed above, where one chooses a physically meaningful operator as a staring vector and cannot chose the number of eigenspaces needed for its eigendecomposition this can play a role in the behavior of the Lanczos sequence, in particular for the point, where the Lanczos sequence should terminate. To investigate this we looked at the tilted-field Ising ring with a local operator as the starting vector. For this example, the starting vector could only be decomposed into eigenvectors of the Liouvillian numerically. To eliminate artifacts due to numerical diagonalization we included an example of a small subspace of the Heisenberg delta chain where the eigendecomposition of the starting vector is known analytically. In both cases, the problem of leaving the Krylov space was observable.

Our own experience suggests that the observed behavior also occurs for schemes that employ Pauli strings [56]. In these schemes, much larger systems can be modelled, however, due to the exponential increase in required computational power and memory the number of achievable iterations is limited to the 15-40 iterations for instance achieved in [36]. It may thus be that the discussed numerical problems which should also occur for the Lanczos coefficients in schemes using Pauli strings are not yet observable at the lower number of iterations.

In addition, it should be noted that the discussed numerical instability also occurs in the usual Lanczos algorithm as demonstrated in the appendix.

ACKNOWLEDGMENT

This work was supported by the Deutsche Forschungsgemeinschaft DFG (355031190 (FOR 2692); 397300368 (SCHN 615/25-2)). We thank Coraline Letouzé, Jiaozi Wang and Jochen Gemmer for valuable discussions.

Appendix A: Example of leaving the subspace for ordinary state Lanczos

In this appendix, we like to show that the problem discussed above arises in ordinary Lanczos procedures where an operator, e.g. the Hamiltonian is applied to a starting vector to generate a Krylov space of which the smallest eigenvalue is taken as an approximation of the true smallest eigenvalue. The failure of the Lanczos procedure can easily be provoked by choosing a starting vector that belongs to an invariant subspace due to a symmetry of the Hamiltonian. If the calculation is not restricted to this subspace but performed in a larger space the dynamics in finite-precision arithmetics generates a sequence of Lanczos vectors that escape the invariant subspace eventually.

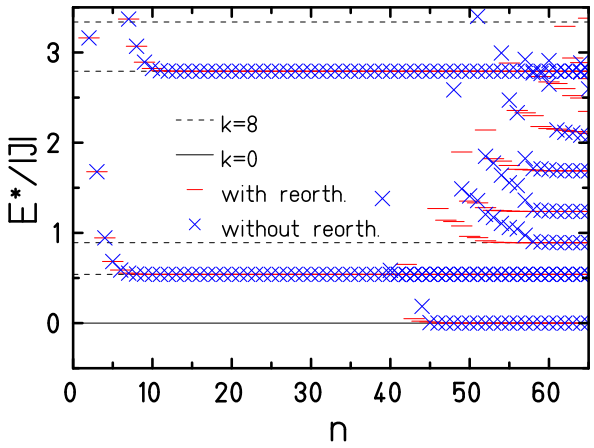

Figure 6. Sequence of (low-lying) energy eigenvalues of T at every Lanczos step n in the vector space with $M = 0$. The dimension of the subspace with $M = 0$ and $k = 8$ is 810, taking additionally into account the spin flip symmetry, the dimension of the subspace with additional odd spin-flip symmetry is 396. The starting vector has got odd symmetry, the ground state even. The solid black line marks the exact ground state energy for $k = 0$; dashed lines mark exact eigenenergies for $k = 8$. The Lanczos sequence with reorthogonalization is depicted by red dashes, the respective sequence without reorthogonalization by blue x-symbols.

In the specific example we consider a quantum spin ring with $N = 16$ and $s = 1/2$ in the Heisenberg model with the same exchange interaction J between nearest neighbors ($-2J$-convention). This system has got several symmetries: $SU(2)$ since it commutes with all components of the total spin, translational symmetry along the ring expressed as C_N point group as well as spin flip symmetry in the subspace with total magnetic quantum number $M = 0$ [57]. We perform the calculation in the subspace with $M = 0$ and choose as starting vector $1/\sqrt{2}(|1010101010101010\rangle - |0101010101010101\rangle)$, which is a superposition of two product states where 0 stands for a local $m_s = 1/2$ and 1 for $m_s = -1/2$. This vector is an eigenstate of the shift operator ($T \equiv C_{16}$) with shift quantum number $k = 8$, whereas the true ground state possesses $k = 0$ [58]. An exact Lanczos procedure should generate a sequence of states that respects the good quantum number $k = 8$.

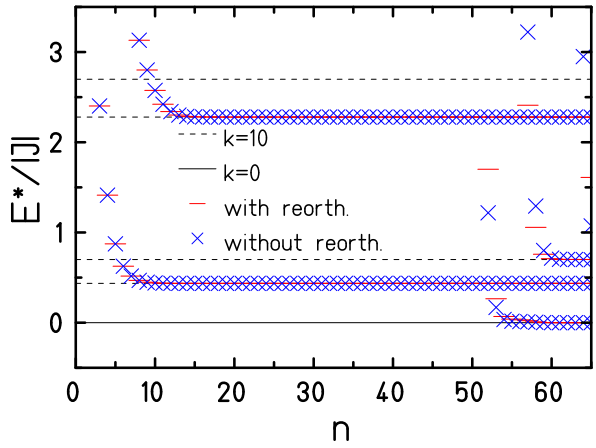

Figure 7. Sequence of (low-lying) energy eigenvalues of T at every Lanczos step n in the vector space with $M = 0$. The dimension of the subspace with $M = 0$ and $k = 10$ is 9252, taking additionally into account the spin flip symmetry, the dimension of the subspace with additional odd or spin-flip symmetry is about half. The starting vector has got odd symmetry, the ground state even. The solid black line marks the exact ground state energy for $k = 0$; dashed lines mark exact eigenenergies for $k = 10$. The Lanczos sequence with reorthogonalization is depicted by red dashes, the respective sequence without reorthogonalization by blue x-symbols.

However, as Fig. 6 demonstrates, in a computer simulation the numerical sequence acquires contributions from states with e.g. $k = 0$. These contributions grow exponentially fast with Krylov space dimension, in particular, in cases they contain the ground state. In the example simulation this happens after about 40 Lanczos steps. Before, the algorithm has accurately found the lowest energy compatible with $k = 8$, but then it develops a component along the overall ground state that belongs to $k = 0$, and within a few steps converges also to the respective eigenvalue. This happens with (red symbols) and and without (blue symbols) reorthogonalization, which once more strengthens our statement that reorthogonalization does not guard against components orthogonal to the true/exact Krylov space.

With Fig. 7 we want to demonstrate that the problem arises after approximately the same number of Lanczos steps and in particular does not scale with the dimension of the underlying spaces. For the example of $N = 20$ spins $s = 1/2$ the dimensions are about ten times larger, but the escape of the Lanczos sequence into the orthogonal complement of the true Krylov space happens after about 50 steps compared to 40 for $N = 16$, see Fig. 6.

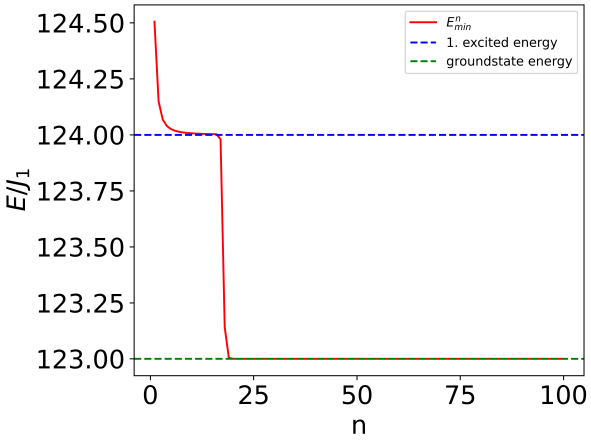

Figure 8. Minimal energies of the tridiagonal matrix for each Lanczos step in the one-magnon subspace of the Heisenberg delta chain with $N = 400$. The analytically known dimension of the Krylov space is $dim(\mathcal{K}) = 101$. The blue and green dashed lines indicate the energy of the first excited and ground state energy respectively.

To further strengthen this finding we again considered the one-magnon subspace of the Heisenberg delta chain (compare section III B). Since we investigate the ordinary state Lanczos we just superimposed all states from the upper band with $k \leq N/4$ for our starting vector, compare Fig. 4. Running the Lanczos algorithm and diagonalizing the tridiagonal matrix in every step leads to the minimal energies seen in Fig. 8. After the minimal energy seems to saturate at the first excited state, as it should, at around $n = 19$ it quickly drops to the ground state energy, even though the initial state should has no overlap with the ground state.

In typical applications in quantum magnetism this problem does not occur because one restricts the vector space to the smallest possible space for the given symmetries. Then, a Lanczos procedure cannot leave this vector space by construction.

[1] C. Lanczos, An iteration method for the solution of the eigenvalue problem of linear differential and integral operators, J. Res. Nat. Bur. Stand. **45**, 255 (1950).

[2] J. Skilling, Maximum entropy and Bayesian methods (Kluwer, Dordrecht, 1988) Chap. The eigenvalues of mega-dimensional matrices, pp. 455–466.

[3] M. Hutchinson, A stochastic estimator of the trace of the influence matrix for Laplacian smoothing splines, Comm. Statist. Simulation Comput. **18**, 1059 (1989).

[4] D. A. Drabold and O. F. Sankey, Maximum entropy approach for linear scaling in the electronic structure problem, Phys. Rev. Lett. **70**, 3631 (1993).

[5] J. Jaklič and P. Prelovšek, Lanczos method for the calculation of finite-temperature quantities in correlated systems, Phys. Rev. B **49**, 5065 (1994).

[6] M. Aichhorn, M. Daghofer, H. G. Evertz, and W. von der Linden, Low-temperature Lanczos method for strongly correlated systems, Phys. Rev. B **67**, 161103(R) (2003).

[7] A. Weiße, G. Wellein, A. Alvermann, and H. Fehske, The kernel polynomial method, Rev. Mod. Phys. **78**, 275 (2006).

[8] H. Avron and S. Toledo, Randomized algorithms for estimating the trace of an implicit symmetric positive semi-definite matrix, J. ACM **58**, 8:1 (2011).

[9] A. K. Saibaba, A. Alexanderian, and I. C. F. Ipsen, Randomized matrix-free trace and log-determinant estimators, Numer. Math. **137**, 353 (2017).

[10] T. Chen, The Lanczos algorithm for matrix functions: a handbook for scientists, arXiv:2410.11090 (2024).

[11] H. D. Simon, Analysis of the symmetric Lanczos algorithm with reorthogonalization methods, Linear Algebra Appl. **61**, 101 (1984).

[12] J. H. Wilkinson, *The algebraic eigenvalue problem*, 1st ed., Monographs on numerical analysis, Oxford science publications (Clarendon Press; Oxford University Press, 1988).

[13] W. Wülling, On stabilization and convergence of clustered Ritz values in the Lanczos method, SIAM J. Matrix Anal. Appl. **27**, 891 (2005).

[14] W. Wülling, The stabilization of weights in the Lanczos and conjugate gradient method, BIT Numer. Math. **45**, 395 (2005).

[15] G. Meurant and Z. Strakoš, The Lanczos and conjugate gradient algorithms in finite precision arithmetic, Acta Numerica **15**, 471 (2006).

[16] F. Roosta-Khorasani and U. Ascher, Improved bounds on sample size for implicit matrix trace estimators, Found. Comput. Math. **15**, 1187 (2015).

[17] J. Schnack, J. Richter, and R. Steinigeweg, Accuracy of the finite-temperature Lanczos method compared to simple typicality-based estimates, Phys. Rev. Research **2**, 013186 (2020).

[18] T. Chen, A. Greenbaum, C. Musco, and C. Musco, Error bounds for Lanczos-based matrix function approximation, SIAM J. Matrix Anal. Appl. **43**, 787 (2022).

[19] T. Chen and G. Meurant, Near-optimal convergence of the full orthogonalization method, Electron. Trans. Numer. Anal. , 421 (2024).

[20] J. M. Deutsch, Quantum statistical mechanics in a closed system, Phys. Rev. A **43**, 2046 (1991).

[21] M. Srednicki, Chaos and quantum thermalization, Phys. Rev. E **50**, 888 (1994).

[22] J. Schnack and H. Feldmeier, Statistical properties of fermionic molecular dynamics, Nucl. Phys. A **601**, 181 (1996).

[23] J. Schnack and H. Feldmeier, The nuclear liquid–gas phase transition within fermionic molecular dynamics, Phys. Lett. B **409**, 6 (1997).

[24] H. Tasaki, From quantum dynamics to the canonical distribution: General picture and a rigorous example, Phys. Rev. Lett. **80**, 1373 (1998).

[25] M. Rigol, V. Dunjko, and M. Olshanii, Thermalization and its mechanism for generic isolated quantum systems, Nature **452**, 854 (2008).

[26] P. Reimann, Foundation of statistical mechanics under experimentally realistic conditions, Phys. Rev. Lett. **101**, 190403 (2008).

[27] A. Polkovnikov, K. Sengupta, A. Silva, and M. Vengalattore, Colloquium, Rev. Mod. Phys. **83**, 863 (2011).

[28] P. Reimann and M. Kastner, Equilibration of isolated macroscopic quantum systems, N. J. Phys. **14**, 043020 (2012).

[29] A. J. Short and T. C. Farrelly, Quantum equilibration in finite time, N. J. Phys. **14**, 013063 (2012).

[30] R. Steinigeweg, A. Khodja, H. Niemeyer, C. Gogolin, and J. Gemmer, Pushing the limits of the eigenstate thermalization hypothesis towards mesoscopic quantum systems, Phys. Rev. Lett. **112**, 130403 (2014).

[31] C. Gogolin and J. Eisert, Equilibration, thermalisation, and the emergence of statistical mechanics in closed quantum systems, Rep. Prog. Phys. **79**, 056001 (2016).

[32] L. D'Alessio, Y. Kafri, A. Polkovnikov, and M. Rigol, From quantum chaos and eigenstate thermalization to statistical mechanics and thermodynamics, Adv. Phys. **65**, 239 (2016).

[33] F. Borgonovi, F. M. Izrailev, L. F. Santos, and V. G. Zelevinsky, Quantum chaos and thermalization in isolated systems of interacting particles, Phys. Rep. **626**, 1 (2016).

[34] M. Schiulaz, M. Tavora, and L. F. Santos, From few- to many-body quantum systems, Quantum Sci. Technol. **3**, 044006 (2018).

[35] P. Reimann and J. Gemmer, Why are macroscopic experiments reproducible? Imitating the behavior of an ensemble by single pure states, Physica A **552**, 121840 (2020).

[36] D. E. Parker, X. Cao, A. Avdoshkin, T. Scaffidi, and E. Altman, A Universal Operator Growth Hypothesis, Phys. Rev. X **9**, 041017 (2019).

[37] M. Schiulaz, E. J. Torres-Herrera, and L. F. Santos, Thouless and relaxation time scales in many-body quantum systems, Phys. Rev. B **99**, 174313 (2019).

[38] Y. Liao, A. Vikram, and V. Galitski, Many-body level statistics of single-particle quantum chaos, Phys. Rev. Lett. **125**, 250601 (2020).

[39] R. Heveling, J. Wang, and J. Gemmer, Numerically probing the universal operator growth hypothesis, Phys. Rev. E **106**, 014152 (2022).

[40] P. Caputa, J. M. Magan, and D. Patramanis, Geometry of Krylov complexity, Phys. Rev. Res. **4**, 013041 (2022).

[41] K. Hashimoto, K. Murata, N. Tanahashi, and R. Watanabe, Krylov complexity and chaos in quantum mechanics,

J. High Energ. Phys. **2023** (11), 40.
[42] E. Rabinovici, A. Sanchez-Garrido, R. Shir, and J. Sonner, Krylov complexity from integrability to chaos, J. High Energ. Phys. **2022** (7), 151.
[43] Q. Hu, W.-Y. Zhang, Y. Han, and W.-L. You, Krylov complexity in quantum many-body scars of spin-1 models, Phys. Rev. B **111**, 165106 (2025).
[44] S. Nandy, B. Mukherjee, A. Bhattacharyya, and A. Banerjee, Quantum state complexity meets many-body scars, J. Phys. Condens. Matter **36**, 155601 (2024).
[45] A. Bhattacharya, P. Nandy, P. P. Nath, and H. Sahu, On Krylov complexity in open systems: an approach via bi-Lanczos algorithm, J. High Energ. Phys. **2023** (12), 66.
[46] P. Nandy, A. S. Matsoukas-Roubeas, P. Martínez-Azcona, A. Dymarsky, and A. del Campo, Quantum dynamics in krylov space: Methods and applications, Phys. Rep. **1125-1128**, 1 (2025).
[47] A. Sánchez-Garrido, On Krylov complexity, arXiv:2407.03866 (2024).
[48] A. Bhattacharya, P. P. Nath, and H. Sahu, Krylov complexity for nonlocal spin chains, Phys. Rev. D **109**, 066010 (2024).
[49] H. G. Menzler and R. Jha, Krylov delocalization/localization across ergodicity breaking, Phys. Rev. B **110**, 125137 (2024).
[50] S. Baiguera, V. Balasubramanian, P. Caputa, S. Chapman, J. Haferkamp, M. P. Heller, and N. Y. Halpern, Quantum complexity in gravity, quantum field theory, and quantum information science, arXiv:2503.10753 (2025).
[51] L. T. Muus, Superoperators, Time-Ordering and Density Operators, in *Electron Spin Relaxation in Liquids: Based on lectures given at the NATO Advanced Study Institute held at "Spåtind," Norway, in August 1971* (Springer US, Boston, MA, 1972) pp. 1–24.
[52] E. Rabinovici, A. Sánchez-Garrido, R. Shir, and J. Sonner, Operator complexity: a journey to the edge of Krylov space, J. High Energ. Phys. **2021** (6), 62.
[53] J. L. F. Barbón, E. Rabinovici, R. Shir, and R. Sinha, On the evolution of operator complexity beyond scrambling, J. High Energ. Phys. **2019** (10), 264.
[54] F. Johannesmann, J. Eckseler, H. Schlüter, and J. Schnack, Nonergodic one-magnon magnetization dynamics of the antiferromagnetic delta chain, Phys. Rev. B **108**, 064304 (2023).
[55] J. Wang, M. H. Lamann, R. Steinigeweg, and J. Gemmer, Diffusion constants from the recursion method, Phys. Rev. B **110**, 104413 (2024).
[56] M. Pieper, *Methods, Problems and Applications of Krylov Complexity*, Master thesis, Bielefeld University, Faculty of Physics (2025).
[57] K. Bärwinkel, H.-J. Schmidt, and J. Schnack, Structure and relevant dimension of the Heisenberg model and applications to spin rings, J. Magn. Magn. Mater. **212**, 240 (2000).
[58] K. Bärwinkel, H.-J. Schmidt, and J. Schnack, Ground state properties of antiferromagnetic Heisenberg spin rings, J. Magn. Magn. Mater. **220**, 227 (2000).